

# Impact of smart transformer voltage and frequency support in a high renewable penetration system

Junru Chen<sup>a,\*</sup>, Muyang Liu<sup>a</sup>, Giovanni De Carne<sup>b</sup>, Rongwu Zhu<sup>c</sup>, Marco Liserre<sup>c</sup>, Federico Milano<sup>d</sup>, Terence O'Donnell<sup>d</sup>

<sup>a</sup> Xinjiang University, Ürümqi, China

<sup>b</sup> Karlsruhe Institute of Technology, Karlsruhe, Germany

<sup>c</sup> Kiel University, Kiel, Germany

<sup>d</sup> University College Dublin, Dublin, Ireland

## ARTICLE INFO

### Keywords:

Smart transformer  
Inertia emulation  
Frequency support  
Voltage support  
High wind penetration

## ABSTRACT

Increasing penetration of power electronics interfaced generation decreases the stability of the system, due to the absence of the rotational inertia in their operation. Emulation of the inertia using converter controls in combination with storages can address this issue. However, this method relies on the use of large quantities of storage to compensate power during a transient power unbalance. Instead of increasing the supply, the smart transformer (ST), with a fast response, offers the possibility to dynamically regulate the demand. This paper investigates the use of an ST to dynamically control reactive power and demand to support voltage and frequency respectively in the grid. The demand is controlled dynamically to emulate inertia. From an analysis based on a 250 kVA, 10kV/400V LV distribution network, it is shown that a demand variation in the range of 6-10% can be achieved. These results are extended to a case study based on the entire all-Island Irish Transmission system which shows that widespread use of STs with these controls could potentially facilitate a 10% increase in wind penetration without the inclusion of any other storage.

## 1. Introduction

The European Commission targets a 40% cut in greenhouse gas emissions compared to 1990 levels and at least a 27% share of renewable energy consumption in 2030 [1]. Many countries with high renewable penetration, such as Denmark, have a considerable exchange capacity with their neighboring power systems. This strong interconnection facilitates the export of power during the overproduction and import of power in case of incidents such as massive disconnection of renewables [2]. On the other hand, other countries such as Ireland, which recently announced a target of 70% of electricity from renewable generation, have a very limited interconnection capacity to its neighbors. For example, Ireland is only interconnected with Northern Ireland via a 1320 MW double circuit tie line and with the United Kingdom via a 500 MW HVDC link [2]. Under such situations, the system must carry significant reserves from conventional generators, from the interruptible load and pumped storage hydroelectricity, in order to reduce the frequency variation and prevent the frequency collapse following the contingency [3]. However, with increasing renewable generation, the conventional generation may become economically unviable and

displaced from the system. Furthermore, power electronics-interfaced renewables, such as wind turbines and PV plants, offer no rotational inertia to the system. This leads to an increase in the rate of change of frequency (RoCoF) that may trigger frequency relays and consequently cause the automatic under-frequency load shedding. This has led to many investigations into alternative sources for flexibility and frequency support in low inertia power systems such as the use of storage and demand response. At a practical level, for example, to provide a financial incentive for the provision of flexibility, the Irish system operator has introduced a range of new system services, such as synchronous inertia and fast frequency response in order to counteract potential issues with frequency stability [4].

Significant attention has also been given to the provision of virtual inertia from the converter interfaced generation. This can be achieved by providing an extra power component proportional to the rate of change of frequency (RoCoF). The required energy can be provided either from the rotational inertia of the wind turbine [5], de-rated operation of the renewable generation [6], or from the co-located electric energy storage system (ESS) [7]. Such approaches have been implemented in wind farms [8,9], PV systems [10] and electric vehicle

\* Corresponding author.

E-mail address: [Junru.chen.1@ucdconnect.ie](mailto:Junru.chen.1@ucdconnect.ie) (J. Chen).

<https://doi.org/10.1016/j.epsr.2020.106836>

Received 17 December 2019; Received in revised form 3 May 2020; Accepted 24 August 2020

Available online 04 September 2020

0378-7796/ © 2020 Elsevier B.V. All rights reserved.

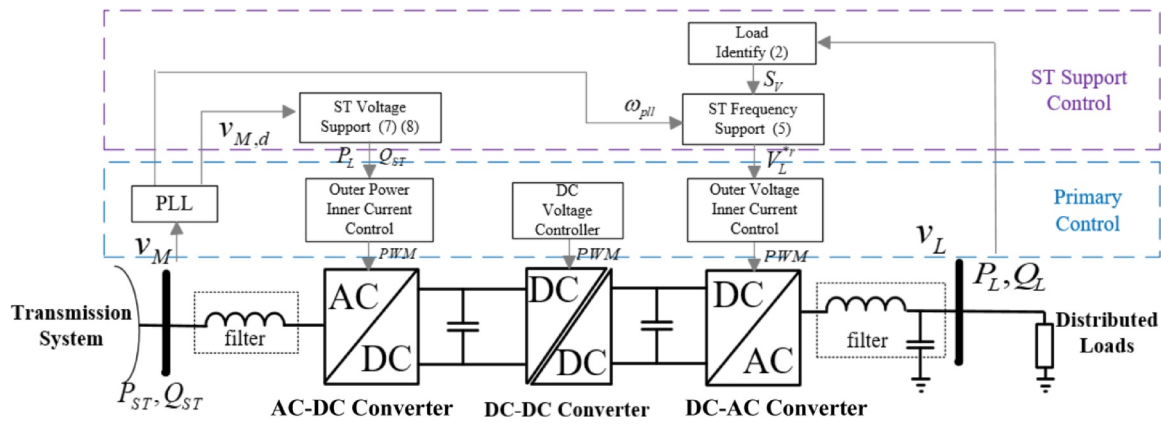


Fig. 1. Smart transformer structure with system support control

charging stations [11]. Obtaining the inertial support from the rotational inertia of the wind turbine implies a recovery period after the contingency where the turbines track back to their maximum power point. De-rated operation of the renewable generation implies a financial cost to the power plant operator. The use of co-located storage to supply the frequency support may require the provision of large quantities of ESS. On the other hand, as back-up regulation to the primary frequency control, contracted load shedding or demand response schemes can be employed and, for example, the Irish system experiences 2.8 such events on average per year [12].

As an alternative approach to the load shedding, frequency support can be provided from the demand by acting on voltage-dependent loads. Following a voltage change, these loads change their power demand, and thus they can represent a controllable resource for providing frequency support in the system. The concept of varying the load consumption by acting on the voltage is not new. Conservation Voltage Reduction (CVR) [13] has already been used in distribution grids for energy saving purposes. Implemented via transformer tap changers, the load demand can be reduced during the peak time for avoiding congestion. However, due to the slow action of the mechanical tap, CVR dynamics are limited. Another application of this concept is based on the use of a Static Var Compensator (SVC) to vary the demand voltage [14]. In this method, to support the frequency, the voltage should typically be reduced after the contingency. However, if a grid voltage dip occurs along with the contingency then the SVC main function of compensating reactive power to maintain the voltage may conflict with a frequency support function. In this paper, a Smart Transformer (ST) is used to provide the voltage regulation. In contrast to the SVC, the ST can perform coordinated and simultaneous voltage and frequency support [15], since its voltage regulation on the primary and secondary side are fully independent.

The ST [16], a power electronics-based transformer [17–20], increases grid controllability, providing grid services without the need for additional hardware [16], this also providing potential for increasing the grid reliability [21]. The main advantage of the ST is that the voltage and reactive power regulation in its primary and secondary side are decoupled [22]. Using this advantage, the ST, in the primary side can independently compensate the reactive power to the transmission system in order to support the grid voltage. In the secondary side, ST can identify the voltage and frequency sensitivity and then control the demand [23], providing services such as: soft load reduction [24], real-time primary frequency regulation [25–27], reactive power compensation [28] and controlled islanding operations [29]. The dynamic control (response time less than 100 ms) of the demand consumption [30] is much faster than the conventional CVR applications, which not only supports the frequency but also improves the transient stability with respect to the inertia provision [15]. Eventually, the ST LV side can be connected also to other distribution feeders, meshing the grid,

and regulating the LV power flow [31]. The device-level analysis of these functions has been well researched in terms of the control design and application [15,23,25,26], and the effects of the ST stability in response to the variable frequency [27]. However, from the system level point of view, there are still unanswered questions such as whether this control can really improve the system stability? or by how much the system stability can be improved with the respect to the penetration of the ST? These questions should be addressed before the widespread application of the ST in grid can be justified.

Although the operation of the ST at the device level has been discussed, studies concerning its impact on the dynamic behavior and stability of the overall power system are lacking. The contribution of this paper is, therefore, to quantify the improvements which widespread use of STs can potentially make to system stability, in terms of frequency, voltage and transient stability under different levels of renewable generation penetration. The levels of demand reduction and reactive power compensation which can be potentially be achieved are firstly quantified on a typical residential distribution system in Manchester, UK. The system stability is then quantified via a case study in the Irish system with different renewable penetration.

The paper is structured as follows: Section 2 reviews the ST topology and its frequency and voltage support functions. Section 3 analyses the frequency support obtained by application of the ST in a 250 kVA, 400 V distribution network. Section 4 provides the simulation results when applied in the all-island Irish transmission system and quantifies the improvement from the control on the system wind penetration, while Section 5 draws the conclusions.

## 2. Smart transformer flexible demand control

The common configuration of the ST is a 3-stage topology consisting of an MV AC/DC primary side converter, MVDC/LVDC converter with a high frequency transformer and LVDC/LCAC secondary side converter as shown in Fig. 1. Besides the MVAC and LVAC ports corresponding to the primary and secondary side of the traditional transformer, this ST topology also has MVDC and LVDC ports, which provide the capability to connect renewable generators, electric vehicle chargers and energy storage system. The MV AC/DC converter connects to the utility grid, uses a PLL to achieve synchronization and applies the conventional decoupled power control to maintain the MVDC voltage. The MVDC/LVDC converter regulates the LVDC voltage, controlling the power flow between two DC links. The LV DC/AC converter supplies the ST-fed grid, controlling the voltage amplitude and frequency. The freedom on the voltage regulation and electric isolation between each port provide the ability of the independent voltage and reactive power control in each port. Consequently, the voltage in the LVAC side can be controlled to vary the demand in a range in response to the frequency and the reactive power in the MVAC side can be controlled to support the

voltage, so that the system stability can be improved. This section reviews these functions.

### 2.1. Load voltage sensitivity identification

The objective of the flexible demand control is to regulate the demand depending on the power system frequency, i.e. reduce the demand in the under-frequency situation while increasing the demand in the over-frequency situation, through load voltage control. To achieve the desired loading power control, the load voltage sensitivity is used to identify the load active power sensitivity to voltage, as described in [23]. Considering an exponential load representation (1), the power is dependent on the voltage as:

$$P_L = P_{L0} \left( \frac{V_L}{V_{L0}} \right)^n \quad (1)$$

where  $P_{L0}$  is the active power demand at nominal voltage  $V_{L0}$ , the exponential value  $n$  is the load voltage coefficient,  $P_L$  is the active power demand at a certain rms voltage  $V_L$ .

The voltage sensitivity  $S_V$ , defined as the percentage power change  $\Delta P_L$  resulting from a percentage voltage change  $\Delta V_L$  as in (2), is used to detect the load voltage coefficient  $n$  in (1).

$$S_V = \frac{\Delta P_L}{\Delta V_L} \approx n \quad (2)$$

When the ST applies the load identification procedure, it purposely applies a 1% trapezoidal voltage disturbance in its LVAC output, measures the power and computes (2) at specified time instants during the voltage variation [24]. It should be noted that the sensitivity identification procedure is independent from the adopted load model, but an exponential model has been adopted due to its simplicity in representing the load response to voltage variations. The load identification step shall be performed anytime that it is deemed necessary (e.g. in response to a significant loading variation), depending on the variability of the identified load. It must be noted that the applied voltage disturbance is small enough that it does not impact on the grid voltage quality.

### 2.2. ST frequency support

This section introduces the basic frequency support control [15], which varies the demand following a grid frequency deviation. As shown in (2), if  $S_V > 0$ , it means demand reduction will result from a voltage reduction, otherwise  $S_V < 0$  means that a demand reduction will result from a voltage increase. Based on this feature, the demand consumption can be shaped to emulate the conventional generators inertial behavior. The available power to support frequency can be determined as:

$$\begin{cases} \Delta P_{L, vmax} = S_V \frac{V_L^* - V_{Lmax}}{V_L^*} \\ \Delta P_{L, vmin} = S_V \frac{V_L^* - V_{Lmin}}{V_L^*} \end{cases} \quad (3)$$

where  $V_{Lmax}/V_{Lmin}$  is the maximum/minimum ST secondary side converter output voltage. To be noted, that the load voltage shall be limited within the range, e.g.,  $(V_L^* \pm 0.1) pu$ , according to EN 50160 [32], where  $V_L^*$  is the voltage nominal value.

The classical swing equation is represented in (4), where  $M$  is the inertia and  $D$  is the turbine governor gain.

$$P_g = M\Delta\dot{\omega}_g + D\Delta\omega_g + P_L \quad (4)$$

In order to mimic the behavior of (4), the flexible demand control based on the voltage and power relationship (3) is proposed in (5). The control links the MV grid frequency, detected by the PLL, to the ST secondary side converter output voltage  $V_L^{*r}$ . The gain  $K_t$  is used to change the secondary side converter voltage according to the RoCoF

$\Delta\dot{\omega}_g$ , while the droop gain  $K_d$  is used to change the voltage proportionally to the frequency deviation  $\Delta\omega_g$ . Finally, the frequency droop and RoCoF terms sum up to determine the ST secondary side converter output voltage reference  $V_L^{*r}$ :

$$V_L^{*r} = \frac{-S_V}{|S_V|} (K_t \Delta\dot{\omega}_g + K_d \Delta\omega_g) + V_L^* \quad (5)$$

where  $K_t \Delta\dot{\omega}_g + K_d \Delta\omega_g$  is the controlled ST secondary side converter voltage change,  $\frac{-S_V}{|S_V|}$  is the relationship (positive or negative) between the voltage change and demand change. Combing (2), (3) and (5), the conventional swing equation (6) is obtained, where  $S_V P_{L0} K_t$  is the virtual inertia and  $S_V P_{L0} K_d$  is the droop gain in system level. Note, the minus sign in (6) indicates that the demand should decrease in the under-frequency situation.

$$P_L = -S_V P_{L0} K_t \Delta\dot{\omega}_g - S_V P_{L0} K_d \Delta\omega_g + P_{L0} \quad (6)$$

It can be seen that from (6), that the emulated inertia depends on the load voltage sensitivity  $S_V$ , loading level  $P_{L0}$  and RoCoF gain  $K_t$ . The load voltage sensitivity  $S_V$  is related to the type of the load, i.e. the residential load voltage sensitivity is 1.2~1.5, the commercial load is 0.99~1.3, and the industrial load is 0.18 [33]. Apparently, applying such control to the residential and commercial loads has more benefit than applying it to the industrial load. The loading level  $P_{L0}$  is the system demand controlled by the ST. It can be concluded that increasing the number of ST-connected residential and commercial loads can potentially improve the system transient and frequency stability.

For the frequency support, in Ireland, the grid code [34] commands that controlled devices, e.g. distributed generators, shall attempt to maximize/minimize active power, when the frequency goes outside the  $50 \pm 2$  Hz, and shall be able to ride through RoCoF of 1.0 Hz/s [35]. Meanwhile, the load voltage variation shall be within  $\pm 0.1 pu$  [32]. Considering these, the ST secondary side converter output voltage should be controlled to the limits  $\pm 0.1 pu$  when either the frequency deviation is 2 Hz (0.04 pu) or the RoCoF is 1.0 Hz/s (0.02 pu/s). Thus, here we suggest  $K_d = 0.1 (pu)/0.04 (pu) = 2.5$  and  $K_t = 0.1 (pu)/0.02 (pu/s) = 5$ . It should be noted that the grid code [33] stipulates also the control dead-bands which for  $\Delta\omega_g$  is 0.2 Hz, and for  $\Delta\dot{\omega}_g$  is 0.02 Hz/s.

### 2.3. ST voltage support

Beside the supply of active power, the ST can use the remaining power capacity  $Q_{ST, max}$ , to inject reactive power for supporting the MV grid voltage. In this respect the ST behaves like a STATCOM [36], with the application of a similar control strategy, i.e. voltage-to-reactive power droop control as in (7).

$$Q_{ST} = K_q (V_M^* - V_{M,d}) + Q_0 \quad (7)$$

$$Q_{ST, max} = \sqrt{S_{ST}^2 - P_L^2} \quad (8)$$

where  $K_q$  is the voltage-to-reactive power droop gain,  $Q_0$  is the initial reactive power injection,  $K_q (V_M^* - V_{M,d})$  is the additional reactive power injection,  $V_M^*$  is the MV side nominal voltage, and  $Q_{ST}$  is the ST total reactive power output to MV grid. The ST priority is delivery of active power  $P_L$  to the load (6), thus, the reactive power compensation is limited according to (8), i.e.  $-Q_{ST, max} \leq Q_{ST} \leq Q_{ST, max}$ .

For the voltage support, the grid code in Ireland commands that the power factor shall be 0.95 leading to lagging, when local voltage deviation is less than 0.1 pu [37]. Thus,  $K_q$  should be selected according to (9) based on the consideration of a maximum 0.95 power factor for the extreme voltage variation, i.e. 0.1 pu.

$$0.1K_q \leq \sqrt{1 - 0.95^2} P_{L0} - Q_0 \quad (9)$$

### 2.4. Discussion

Eqs. 2–(9) construct the flexible demand control as shown in Fig. 1. Hence, by dynamically controlling the demand and compensating reactive power, this control can improve the system transient frequency and voltage stability.

The flexible demand control is used to support the system stability under transients only, and not to purposely raise the voltage or lower the demand to change the static system power flow. In other words, the purpose of this control is to improve the system stability and reduce the occurrence of load shedding.

Some of the load in practice may present a dynamic recovery response, e.g. thermostatically controlled loads, which can appear as impedance loads in a short timeframe, and as constant power loads in the longer timeframe. Typically, the recovery time of this kind of load is around 2 min [38], while the proposed control focuses on the fast response and primary control in the time range of seconds. The load recovery of thermostatically controlled loads is still required to be compensated by the generators via a secondary regulation. The flexible demand control is purposely not designed to achieve zero steady-state frequency and voltage error, in order to activate the secondary control of the generators. It is assumed that this secondary control will return the system frequency to its nominal value and consequently bring the control of the ST backs to the nominal state as well. The focus of the control on the inertia support at the beginning of the contingency where both  $\Delta\omega_g$  and  $\Delta\dot{\omega}_g$  are considerable, i.e. the frequency nadir in the first swing and large initial RoCoF. This provides an alternative way to avoid building extensive storages in the system to offer the fast frequency response. The paper emphasizes the quantification of the system stability improvement by the inclusion of the ST, thus, it only shows the results in the time scale of the primary control and the load in the remainder of the paper is modeled as an exponential load.

### 3. Distribution system analysis

In order to quantify the demand flexibility available from a typical distribution system, the proposed flexible demand control is applied to, a 250 kVA, 10 kV/400 V (based on an ENWL distribution network in Manchester, UK, [39]) consisting of total 90 residential customers evenly distributed across three phases, with 32, 26 and 32 customers in phase A, B and C respectively. The network is shown in Fig. 2 [40] and is divided into three areas, only for the purposes of presentation of unbalanced and stochastic load data as given in Fig. 3. Each load has been assigned different data independently. The load is modeled as an exponential load (1) with its winter daily loading profile  $P_{Lo}$  at the

feeder terminal given in Fig. 3 [40]. The load data has a one-minute resolution and the system power flow for each one minute is solved by the Matlab *fsolve* function. The simulation first verifies the load voltage sensitivity identification method by purposely introducing a 1% voltage reduction and using (2) to compute the sensitivity. Based on this, it quantifies the available active and reactive power which can be used to support the grid stability from this distribution system.

Fig. 4 shows the results of the voltage sensitivity identification. The cyan line shows the result from computing the sensitivity every 1 min. However, the voltage sensitivity does not need to be computed frequently, but only needs to be re-computed when the load undergoes a significant change. Fig. 4 also shows the voltage sensitivity which results from re-computing in response to a load change  $\Delta P$  of greater than 20%, 40% and 60%. The increase in computation threshold reduces the computation frequency but also reduces the precision as a trade-off. For example, when the threshold for re-computing is set at 60%, the load identification only needs to be done 7 times daily. The proposed flexible demand control does not require a precise voltage sensitivity to be effective but only needs the sign of the  $S_V$  to avoid an adverse demand regulation, thus, a reasonable setting may be to re-compute for a 40% threshold resulting in 18 load identification steps in a day.

In the distribution system, due to the line impedance and its consequent voltage drop, the end-line load voltage is commonly the minimum voltage in the network and should not fall outside the range of 0.9 to 1.1 pu, according to the EN 50160 standard. Thus, the minimum ST secondary side converter voltage used to support frequency in (3) should consider the end-line load voltage and should dynamically change with the loading variation. Reference [30] introduces the method to determine the minimum supply voltage linked to the loading in the distribution system. In the ST application, Fig. 5 shows the possible ST secondary side converter voltage range for the grid under investigation. Correspondingly, Fig. 6 (a) shows the load active power variation range, and Fig. 6 (b) shows the available active power, used to support the frequency, as a percentage of the nominal situation, where “demand reduction” corresponds to the minimum voltage in under-frequency and “demand increase” corresponds to the maximum voltage in over-frequency. Since the minimum voltage is variable and greater than 0.9 pu but the maximum voltage is a constant 1.1 pu, the power (on average 6%) used to support the under-frequency situation is lower than that (on average 10%) used to support an over-frequency situation from the same distribution system.

The ST rating matches the distribution network maximum apparent power consumption i.e. 250 kVA. The active power delivery under different voltage situations is given in Fig. 6 (a), while the remaining power capacity can be used to compensate the reactive power into the

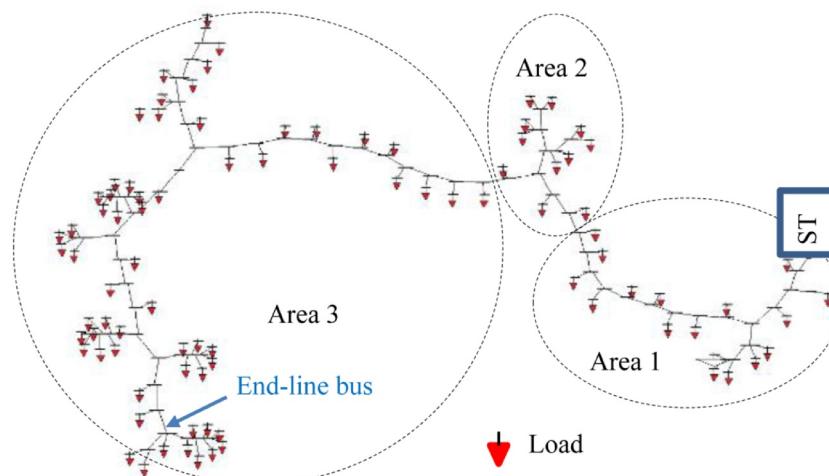


Fig. 2. ENWL distribution network in Manchester.



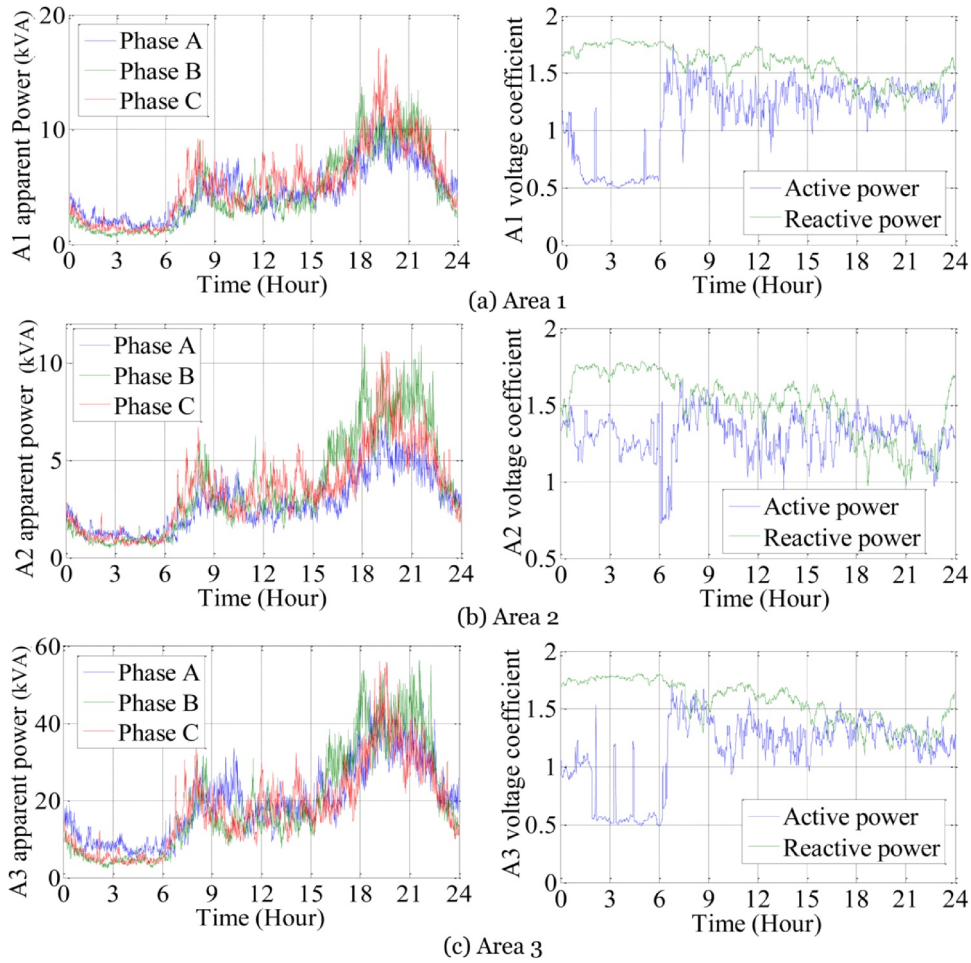


Fig. 3. Winter daily three phase loading profile in area 1, 2 and 3.

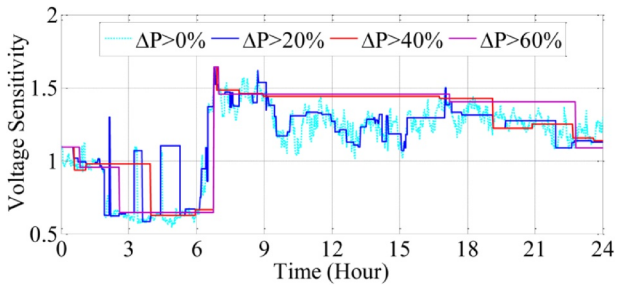


Fig. 4. Load voltage sensitivity identification of the distribution network.

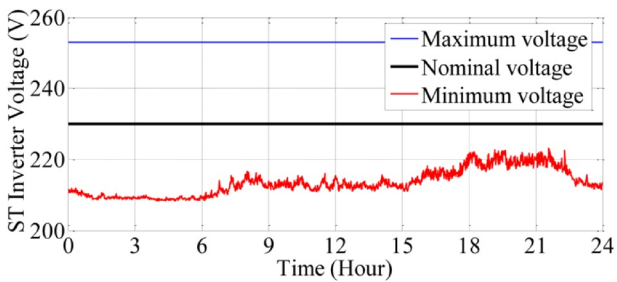


Fig. 5. Safety network supply voltage range.

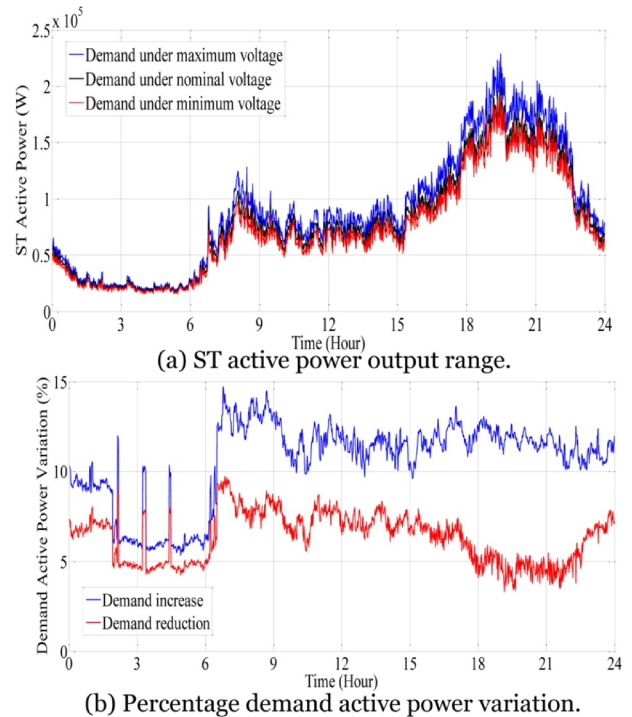


Fig. 6. Available load active power for frequency support.

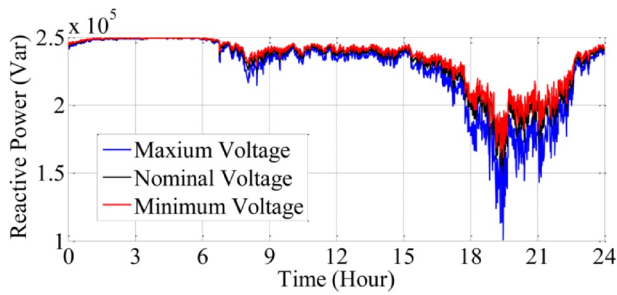


Fig. 7. Available ST reactive power for voltage support.

utility grid for voltage support purposes, as shown in Fig. 7. It can be seen that the available reactive power is limited during peak demand time to nearly 150 kVar or 0.6 pu, and the reduction in the voltage or demand can provide more available reactive power to support voltage. This interaction is favorable with the distributed load voltage sensitivity  $S_V > 0$ , because a frequency reduction normally requires a voltage reduction, so that the reduced demand  $P_L$  in (8) allows an increase in the feasible reactive power compensation  $Q_{ST, max}$ .

#### 4. Case study in all-island Irish transmission system

The previous section characterized the level of frequency and voltage support which might be available from a single distribution system. This section extrapolates this support to an entire power system to attempt to quantify the potential benefit at the transmission system level. The Irish power system is considered as a case study. It should be noted that, in the following case studies, the STs work in the closed loop with the main power system, where their active and reactive power demand influence the main power system voltage and frequency, and vice versa.

The Irish Transmission system grid data is provided by EirGrid, the Irish TSO, consisting of 1,479 buses, 1,851 transmission lines and transformers, and 245 loads as shown in Fig. 8. The model is built into Dome, a Python-based power system software tool [41]. There are 21 conventional synchronous power plants modeled as 6th order synchronous machine models with automatic voltage regulators and turbine governors, 6 power system stabilizers, and 176 wind power plants, of which 142 are doubly-fed induction generators and 34 direct drive wind turbines achieving 40.97% wind penetration (WP). This model provides a dynamic representation of the actual Irish electrical grid with accurate topology and load data. It should be noted that the dynamic data of generators are not the actual generator data but can reflect the real Irish system dynamics. The details of the device models are given in [42]. The consumption of electricity in Ireland is shared by 31.4% in residential, 26.9% in commercial and 39.3% in industrial loads in 2015 [43].

For the purposes of the whole system level simulation, the aggregated effect of all of the MV/LV STs is represented as STs interfaced between the transmission system and the loads. Due to the lack of any DC grid in Irish system, the DC connections of the ST are neglected. The model of the ST used is based on the differential-algebraic equation model in [44] and has been validated via a comparison with results from hardware-in-the-loop experiment [45]. The ST size or capacity is set as 100% of initial loading. The settings for the proposed flexible demand control are the ones identified in Section 2. The load connected through the ST is modeled as an exponential load with voltage coefficient 1.5 for residential loads and 1.0 for commercial loads [33]. The grid frequency is measured locally in each of the ST. As a contingency in the case study, the HVDC line to the United Kingdom, which represents the largest infeed to the system, disconnects at 1 s while importing 0.4 GW. The overall system load at this time is 2.36 GW.

We investigate two cases. Case 1 considers the effect of the ST

flexible demand control on the system voltage and frequency after the contingency, if the residential and/or commercial load is controlled by the ST with the flexible demand control. Case 2 and 3 quantify frequency and voltage stability respectively under an increase in wind penetration. The aim of these cases is to quantify the extra level of non-synchronous generation allowable, from the perspective of frequency and RoCoF limits, assuming the load is ST controlled.

##### 4.1. Case 1: voltage/frequency control in Irish grid

In this case, we first apply the ST with flexible demand control to the residential load only, as its voltage coefficient is the highest [33], and then additionally apply the ST to the commercial load, compared with the original system with no ST. Fig. 9 shows (a) the grid frequency and (b) the bus voltage at the capital city, Dublin, after contingency.

It can be seen from Fig. 9 (a) that the proposed control can improve the system frequency response after the contingency, especially as regards RoCoF reduction. Because there is sufficient primary control from the generation, the ST control has limited benefit on the frequency deviation in this case. It can also be seen that the application of the ST to the residential loads has the largest effect with an additional smaller effect from the commercial loads, which is due to the residential loads having higher voltage coefficient and load occupation, thus contributing higher inertia as explained in (6).

From Fig. 9 (b), it can be seen that the reactive power compensation from the ST can improve the voltage response after the contingency. It is worth noting that the voltage behavior at the instant of the contingency (1-1.5 s) for each scenario is similar, this is because the available reactive power during this period is limited due to the converter capacity limit. However, following the frequency reduction, the proposed control reduces the loading which frees converter capacity for reactive power compensation. Thus, after 1.5 s the voltage response improves.

##### 4.2. Case 2: frequency stability in high wind penetration

In this case, the possible maximum wind penetration while maintaining frequency stability, in the Irish system with the flexible demand control under the same contingency (loss of the HVDC line) is investigated. The Irish grid code requires that the frequency deviation shall remain within a  $\pm 2$  Hz range and limits RoCoF to 1 Hz/s in the first 500 ms and 0.5 Hz/s calculated over 500 ms [35]. In order to increase the wind penetration, the SGs are gradually replaced by the direct drive WG thus also losing their frequency and voltage support functions. For each wind penetration level, simulations similar to those in Fig. 11 are performed. The frequency nadir, RoCoF in the first 500 ms and steady-state value are recorded and plotted in Fig. 10.

From Fig. 10 (a), the increase in WP reduces the frequency nadir and increases the RoCoF due to the reduction of the system inertia. The proposed control, if it is applied on both residential and commercial load, has considerable improvements on the frequency nadir. However, when the WP reaches around 85%, this improvement becomes negligible as the available frequency response is simply inadequate to compensate for the reduced system inertia. This indicates that the supports from the load aspects is limited, and the achievement for 100% WP should still rely on the renewable generator controls. As a result, in relation to limiting the frequency nadir within  $\pm 2$  Hz or 48 Hz, the proposed control applied to residential load can improve the WP from 73.1% to 83.96% but applying it to the additional commercial load has only a slight improvement, increasing from 83.96% to 84.88%. This is because the voltage sensitivity of the residential load is higher than the commercial load, and the application of the ST in the residential load can obtain the maximum benefits on the system frequency and transient stability. The additional application on the commercial load is not very appreciable compared with its expensive installation cost.

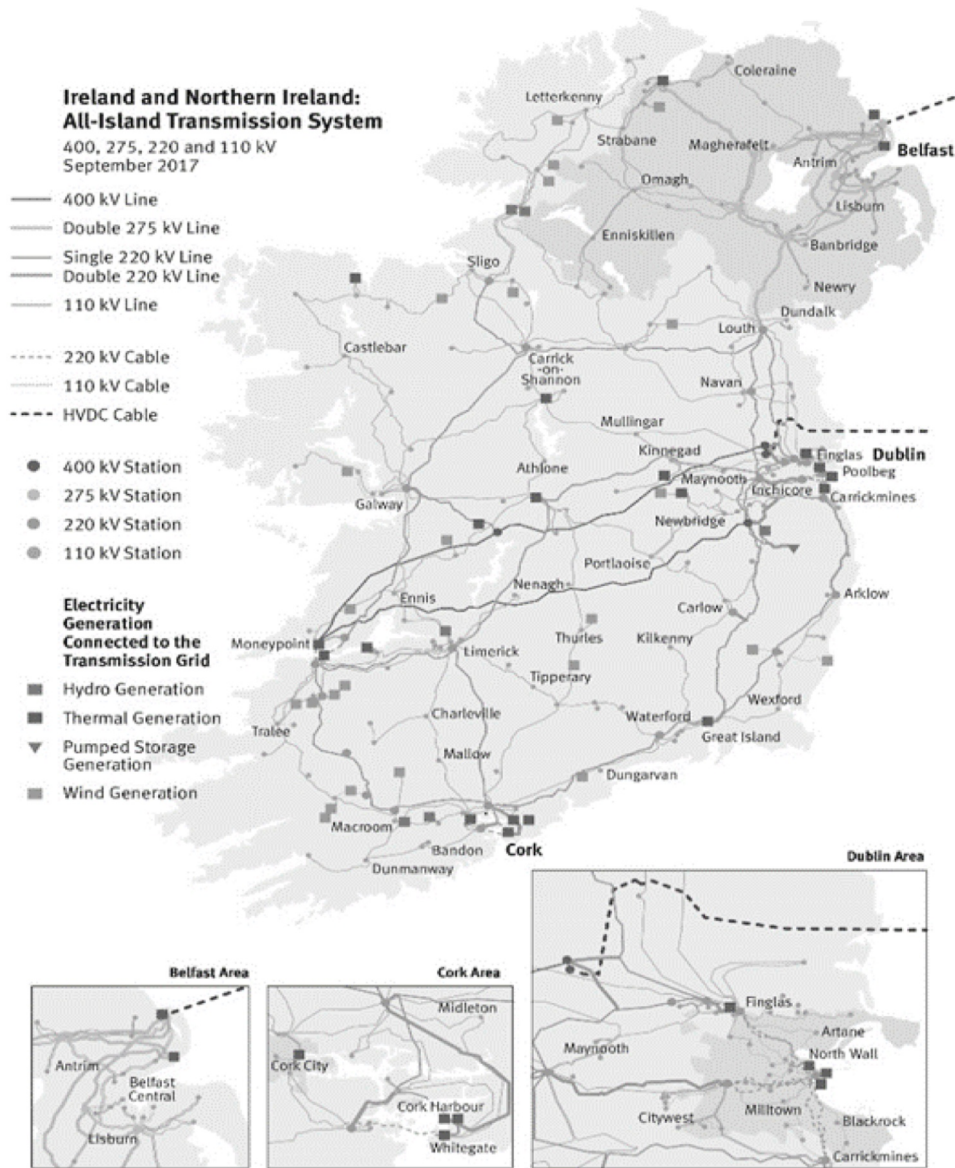


Fig. 8. All-island Irish power system map (available at: [www.eirgridgroup.com](http://www.eirgridgroup.com)).

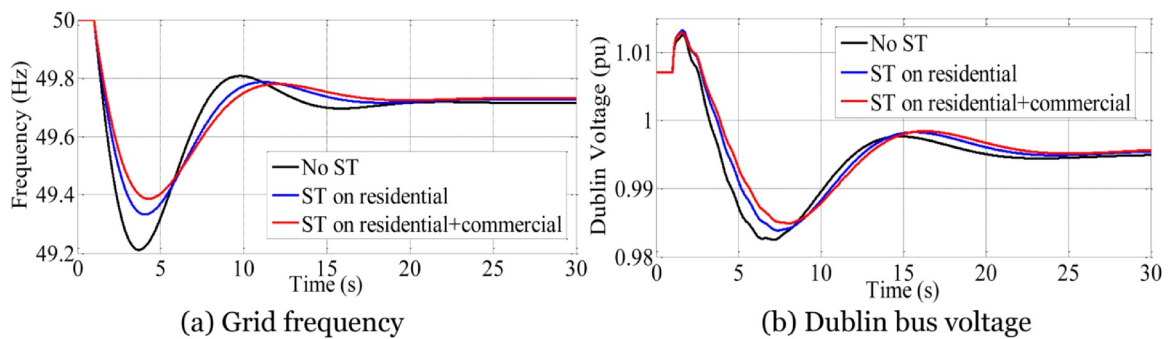


Fig. 9. Case 1 results.

On the other hand, regarding the RoCoF limit of 1 Hz/s, the maximum WP for the no ST case is constrained to 63.49%, while in this case, the use of the proposed control can push the WP to 72.96% and 77.61% corresponding to the ST control applied to residential loads or additionally commercial loads (Fig. 10(b)).

With the replacement of SGs by wind generators, turbine governor

response is being removed and hence the steady-state frequency in Fig. 10 (c) is decreasing with the WP increase. The ST frequency support in the steady state is limited, up to 6% for the residential load for a 2 Hz frequency deviation, and is linked to the steady-state frequency with a droop gain. Therefore, the application of the ST can improve the steady-state frequency deviation. However, even at the highest wind



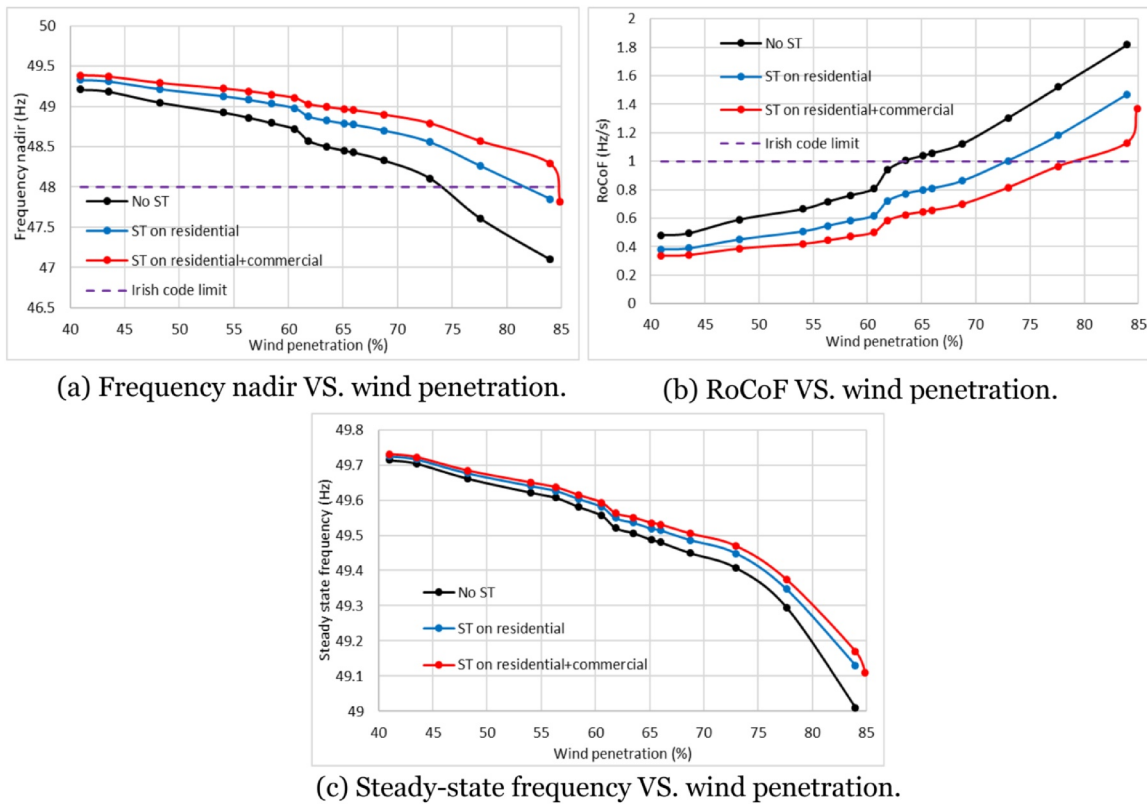


Fig. 10. Case 2 results.

penetration, the worst frequency deviation is 1 Hz, which corresponds to 3% load reduction in ST controlled load, so that the steady-state frequency improvement is very little, only 0.1 Hz, from the application of the ST.

In total, considering the nadir and RoCoF limits resulting from the loss of the largest infeed, the proposed control could increase the WP by approximately 10% WP in the Irish system without the use of any additional storage. However, in order to keep the same steady-state frequency, the inclusion of extra power support is required. This reflects the fact that the inclusion of the ST with such control has more benefits in terms of inertia support with respect to the RoCoF and frequency nadir improvement, rather than the frequency support.

#### 4.3. Case 3: voltage stability in high wind penetration

In this case, we focus on the voltage stability in the case of the increase in WP. To investigate the impact of the reactive power compensation from the ST alone, the WGs do not implement any voltage-to-reactive-power-droop control, i.e. they behave like a constant power source. Therefore, the WP increase and the associated decrease in SG AVR response results in the voltage at the Dublin bus decreasing in both nadir and steady-state value as shown in Fig. 11.

It can be seen in Fig. 11 (a) that the application of the ST results in only a slight improvement in the voltage nadir, on average 0.005 pu, considerably less than the effect on the frequency nadir. This is because the voltage support is mainly dependent on its local reactive power compensation while the frequency support is global. This is also the reason that the voltage nadir reduces in a less consistent manner and it is dependent on the location of the replaced SG, unlike the frequency nadir which shows consistent reduction with the gradual increase in WP.

As shown in Fig. 11 (b), the steady-state voltage tendency is similar with the steady-state frequency tendency in this process. This is owing to the voltage to reactive power droop compensation in the ST. The

lower the steady-state voltage, the higher the reactive power compensation, and thus, improvements from the application of the ST become significant.

## 5. Conclusions

The fast response ST enables the demand to be dynamically controlled in the same manner as inertia emulation and droop control applied to storage, to support voltage and frequency in the grid. Through the analysis and quantification of the control applied to a typical distribution system and scaled to a case study of the entire Irish system, the following conclusions can be drawn: i) The flexible loading used to support frequency from a typical residential area (for example, an ENWL distribution network in Manchester, UK) is approximately 6% for an under-frequency situation, and 10% for an over-frequency situation. Meanwhile, the available reactive power capacity can be used to support voltage, depending on the loading level but at least to 0.6 pu. ii) The application of the ST with such control can provide considerable inertia into the system from the case study based on the Irish system, which can help improve by 10% the allowable level of non-synchronous wind generation without the addition of other inertia emulation while maintaining the same transient stability level. iii) The ability of this ST control to provide steady-state support (primary regulation) is limited due to the limitations in load response. In addition, the contribution of the voltage stability improvement is poor when the loading is heavy as indicated in the paper. For longer duration frequency support, the proposed control would have to work in combination with other sources of frequency and voltage support in the system in the case of large penetrations of non-synchronous generation.

Although this study supports the technical feasibility, the important question still remains regarding the commercial feasibility of the widespread use of STs in the power system. Ultimately a larger system investment planning study would be required in order to investigate the commercial advantages of the ST solution for the provision of system



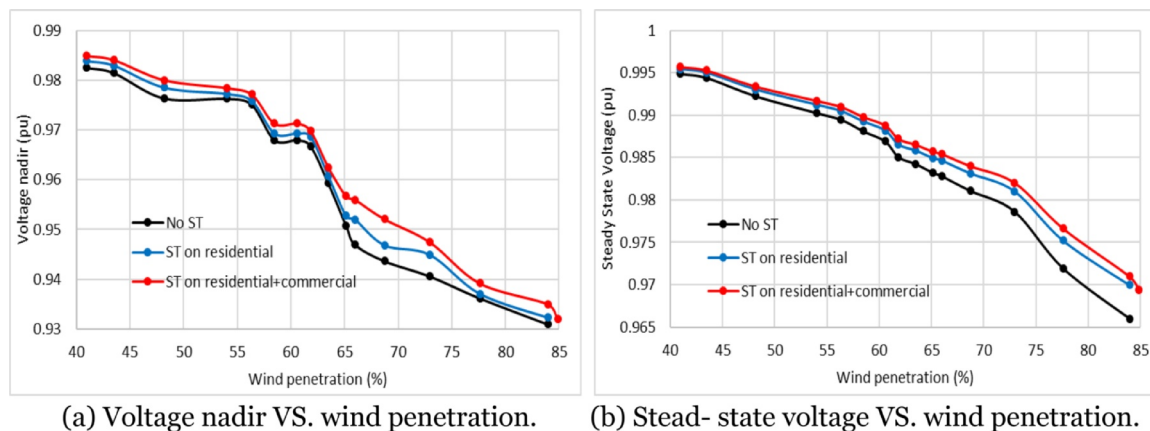


Fig. 11. Case 3 results.

services compared to alternatives. Such a study should consider realistic projections for the capital cost of the ST, the complete set of services which it can provide and the cost of provision of such services by other means (demand response, STATCOMs, storage, etc). This remains as future work, but the work in this paper is seen as providing a basis in that it attempts to quantify some of the flexibility available from the ST.

**CRedit authorship contribution statement**

**Junru Chen:** Conceptualization, Methodology, Software, Validation, Formal analysis, Writing - original draft. **Muyang Liu:** Methodology, Software. **Giovanni De Carne:** Conceptualization, Writing - review & editing. **Rongwu Zhu:** Writing - review & editing. **Marco Liserre:** Writing - review & editing, Supervision. **Federico Milano:** Resources, Data curation, Writing - review & editing, Supervision. **Terence O'Donnell:** Writing - review & editing, Supervision, Funding acquisition.

**Declaration of Competing Interest**

None.

**Acknowledgments**

This work is funded by the Science Foundation Ireland (SFI) Strategic Partnership Programme Grant Number SFI/15/SPP/E3125, SFI/15/IA/3074, the European Research Council (ERC) under grant 616344 HEART, and the Ministry of Science, Research and the Arts of the State of Baden-Wuerttemberg Nr. 33-7533-30-10/67/1. Junru Chen and Federico Milano are partly funded by the European Commission, under the project EdgreFLEx, grant no. 883710.

**References**

[1] European Commission, "A policy framework for climate and energy in the period from 2020 to 2030" Brussels, 22, Jan. 2014.  
 [2] N. Aparicio, et al. "Automatic under-frequency load shedding mal-operation in power systems with high wind power penetration," Elsevier, May 23, 2016.  
 [3] J. Machowski, J.W. Bialek, J.R. Bumby, *Power System Dynamics: Stability and Control*, Second edition, John Wiley & Sons, Inc., 2008.  
 [4] EirGrid and SONI, "DS3 system services qualification trials process outcomes and learnings 2017," 6 Nov. 2017.  
 [5] L. Zeni, A. Rudolph, J. Münster-Swendsen, I. Margaris, A. Hansen, P. Sørensen, Virtual inertia for variable speed wind turbines, *Wind Energy* 16 (8) (2013) 1225–1239.  
 [6] H. Xin, Y. Liu, Z. Wang, et al., A new frequency regulation strategy for photovoltaic systems without energy storage, *IEEE Trans. Sustain. Energy* 4 (4) (2013) 985–993.  
 [7] S. Arco, J.A. Suul, O.B. Fosso, A virtual synchronous machine implementation for distributed control of power converters in smart grids, *Electr. Power Syst. Res.* 122 (May 2015) 180–197.

[8] Y. Ma, W. Cao, L. Yang, F. Wang, L. Tolbert, Virtual synchronous generator control of full converter wind turbines with short-term energy storage, *IEEE Trans. Ind. Electron.* 64 (11) (Nov. 2017) 8821–8831.  
 [9] L. Huang, et al., Synchronization and frequency regulation of DFIG-based wind turbine generators with synchronized control, *IEEE Trans. Energy Convers.* 37 (3) (Sept. 2017) 1251–1262.  
 [10] Q-C. Zhong, Z. Ma, W. Ming, G.C. Konstantopoulos, Grid-friendly wind power systems based on the synchronverter technology, *Energy Convers. Manage.* 89 (1 Jan. 2015) 719–726.  
 [11] J.A. Suul, S. D'Arco, G. Guidi, Virtual synchronous machine-based control of a single-phase bi-directional battery charger for providing vehicle-to-grid services, *IEEE Trans. Ind. Appl.* 52 (4) (July-Aug. 2016) 3234–3244.  
 [12] Soni and Eirgrid, All-Island Transmission System Performance Report, (2017).  
 [13] P. Sen, K. Lee, Conservation voltage reduction technique: an application guideline for smart grid, *IEEE Trans. Ind. Appl.* 52 (3) (May/June 2016).  
 [14] Y. Wan, M.A.A. Murad, M. Liu, F. Milano, Voltage frequency control using SVC devices coupled with voltage dependent loads, *IEEE Trans. Power Syst.* 34 (2) (March 2019) 1589–1597.  
 [15] J. Chen, et al., Smart transformer for the provision of coordinated voltage and frequency support in the grid, *IECON 2018 - 44th Annual Conference of the IEEE Industrial Electronics Society*, Washington, DC, 2018, pp. 5574–5579.  
 [16] L. Ferreira Costa, G. De Carne, G. Buticchi, M. Liserre, The smart transformer: a solid-state transformer tailored to provide ancillary services to the distribution grid, *IEEE Power Electron. Mag.* 4 (2) (June 2017) 56–67.  
 [17] A.Q. Huang, M.L. Crow, G.T. Heydt, J.P. Zheng, S.J. Dale, The future renewable electric energy delivery and management (FREEDM) system: the energy internet, *Proc. IEEE* 99 (1) (Jan. 2011) 133–148.  
 [18] X. She, X. Yu, F. Wang, A.Q. Huang, Design and demonstration of a 3.6-kV–120-V/10-kVA solid-state transformer for smart grid application, *IEEE Trans. Power Electron.* 29 (8) (Aug. 2014) pp.3982–pp.3996.  
 [19] F. Ruiz, M.A. Perez, J.R. Espinosa, T. Gajowik, S. Stynski, M. Malinowski, Surveying solid-state transformer structures and controls: providing highly efficient and controllable power flow in distribution grids, *IEEE Ind. Electron. Mag.* 14 (1) (March 2020) 56–70.  
 [20] M.A. Hannan, State of the art of solid-state transformers: advanced topologies, implementation issues, recent progress and improvements, *IEEE Access* 8 (2020) 19113–19132.  
 [21] E. Pourmaras, J. Espejo-Urbe, Self-repairable smart grids via online coordination of smart transformers, *IEEE Trans. Ind. Inf.* 13 (4) (Aug. 2017) 1783–1793.  
 [22] M.T.A. Khan, A.A. Milani, A. Chakraborty, I. Husain, Dynamic modeling and feasibility analysis of a solid-state transformer-based power distribution system, *IEEE Trans. Ind. Appl.* 54 (1) (Jan.-Feb. 2018) 551–562.  
 [23] G.D. Carne, M. Liserre, C. Vournas, On-line load sensitivity identification in lv distribution grids, *IEEE Trans. Power Syst.* 32 (2) (March 2017) 1570–1571.  
 [24] G. De Carne, G. Buticchi, M. Liserre, C. Vournas, Load control using sensitivity identification by means of smart transformer, *IEEE Trans. Smart Grid P* (99) (Oct. 3, 2016).  
 [25] G. De Carne, G. Buticchi, M. Liserre and C. Vournas, "Real-time primary frequency regulation using load power control by smart transformers," *IEEE Trans. Smart Grid, Early Access*.  
 [26] J. Chen, R. Zhu, T. O'Donnell, M. Liserre, Smart transformer and low frequency transformer comparison on power delivery characteristics in the power system, 2018 AEIT International Annual Conference, Bari, 2018, pp. 1–6.  
 [27] Z. Zou, G. De Carne, G. Buticchi, M. Liserre, Smart transformer-fed variable frequency distribution grid, *IEEE Trans. Indust. Electron.* 65 (1) (Jan. 2018) 749–759.  
 [28] D.G. Shah, M.L. Crow D, Online volt-var control for distribution systems with solid state transformers, *IEEE Trans. Power Deliv.* 31 (1) (Feb. 2016) 343–350.  
 [29] M. Couto, J.A. Peças Lopes, C.L. Moreira, Control strategies for multi-microgrids islanding operation through smart transformers, *Electr. Power Syst. Res.* 174 (2019).  
 [30] J. Chen, C. O'Loughlin, T. O'Donnell, Dynamic demand minimization using a smart

- transformer, Proc. 43rd Annual Conference of the IEEE Industrial Electronics Society, Beijing, China, IECON 2017, Dec. 2017, pp. 4253–4259.
- [31] D. Das, H. V M, C. Kumar and M. Liserre, "Smart transformer enabled meshed hybrid distribution grid," in IEEE Trans. Indust. Electron..
- [32] Copper Development Association, Voltage disturbances standard EN 50160- voltage characteristics in public distribution systems, Power Quality Application Guide, (July 2004).
- [33] Electric Power Research Institute, "Measurement-based load modelling," CA: 2006. 1014402.
- [34] EirGrid, "EirGrid grid code version 6.0," 22 July 2015.
- [35] EirGrid and SONI, RoCoF Alternative & Complementary Solution Project, Phase 2 Study Report, (31 March, 2016).
- [36] X. Gao, G. De Carne, M. Liserre, C. Vournas, Voltage control by means of smart transformer in medium voltage feeder with distribution generation, Power Tech. (2017) 20 Jul. 2017.
- [37] ESB Networks, "The distribution system security and planning standards," Jan. 2015.
- [38] Romero Navarro, Dynamic Load Models for Power Systems, 'Estimation Of Time-Varying Parameters During Normal Operation', Licentiate Thesis Lund University, Department of Industrial Electrical Engineering and Automation, 2002.
- [39] I. Ibrahim, V. Rigoni, C. Loughlin, Jasmin S, T. Donnell, Real-time simulation platform for evaluation of frequency support from distributed demand response, Cigre Symposium, Dublin, 2017.
- [40] J. Chen, T. Yang, C. Loughlin, T.M. O'Donnell, Neutral current minimization control for solid state transformers under unbalanced loads in distribution systems, IEEE Trans. Indust. Electron. (Dec. 2018).
- [41] F. Milano, A Python-based software tool for power system analysis, IEEE PES General Meeting, Vancouver, Canada, 21-25 July 2013.
- [42] F. Milano, Power System Modelling and Scripting, Springer, London, August 2010.
- [43] M. Howley and M. Holland, "Energy in Ireland 1990-2015," Sustainable Energy Authority Of Ireland (SEAI), Nov. 2016.
- [44] M. Khan, A. Milani, A. Chakraborty, I. Husain, Dynamic modeling and feasibility analysis of a solid-state transformer-based power distribution system, IEEE Trans. Ind. Appl. 54 (1) (Jan/Feb. 2018).
- [45] Y. Tu, J. Chen, H. Liu, T. O'Donnell, Smart Transformer Modelling and Hardware in-the-loop Validation, 2019 IEEE 10th International Symposium on Power Electronics for Distributed Generation Systems (PEDG), Xi'an, China, 2019, pp. 1019–1025.